Antiferromagnetism in 4*d* transition metals

V. L. Moruzzi and P. M. Marcus
IBM Research Division, Thomas J. Watson Research Center, P.O. Box 218, Yorktown Heights, New York 10598
(Received 31 July 1990)

Total-energy band calculations employing a fixed-spin-moment procedure and the augmented-spherical-wave method are used to study the volume dependences and existence ranges of antiferromagnetic behavior in the 4*d* transition metals constrained to cubic lattices. At expanded volumes we find stable antiferromagnetic solutions of the Kohn-Sham equations for bcc niobium, molybdenum, and technetium, and for fcc technetium, and metastable antiferromagnetic solutions for fcc ruthenium. We find no stable antiferromagnetic solutions for fcc rhodium or palladium. Comparisons are made with the occurrence of antiferromagnetism in the 3*d* transition metals.

I. INTRODUCTION

Although there are no known experimental occurrences of ground-state ferromagnetic or antiferromagnetic order in the 4*d* transition metals, some of these metals are known to exhibit incipient magnetic behavior and large paramagnetic susceptibilities, implying sensitive volume-dependent magnetic properties. Indeed, fixed-spin-moment total-energy band calculations[1] for fcc rhodium and palladium show[2] calculated magnetic susceptibilities that increase with volume and become singular at well-defined critical volumes which mark the beginning of ferromagnetic behavior. This onset of ferromagnetism at expanded volumes is the expected behavior of all normally nonmagnetic transition metals and can be understood in terms of increased importance of exchange lowering of the total energy by electron polarization as the volume of the system increases. With increasing volume (or decreasing density), atomic separations increase and electronic interactions diminish, tending towards the free-atom limit and the Hund's-rule spin value. At some critical volume, the system can achieve a lower energy by spin splitting the bands. First-principles total-energy band calculations have demonstrated[3] the existence of system-dependent critical volumes marking the onset of magnetic behavior for all of the 3*d* and 4*d* transition metals.

Antiferromagnetism is fairly common in the 3*d* transition metals, especially at expanded volumes. Our comprehensive first-principles survey of the eight 3*d* transition metals in the bcc and fcc structures shows[4,5] that out of the 16 possibilities, there are five cases with antiferromagnetic solutions at some volume. These cases all occur in the middle of the transition series where the *d* bands are nearly half full and where one-atom-cell calculations yield first-order magnetovolume transitions from nonmagnetic to ferromagnetic behavior. Similarly, we might expect to find the most favorable conditions for antiferromagnetism in the 4*d* transition metals in systems with nearly half-filled *d* bands. This paper extends our survey of antiferromagnetism to the 4*d* transition metals in the bcc and fcc structures and shows this expectation to be correct.

From a band-theoretical point of view, antiferromagnetic order can be studied simply by increasing the size of the unit cell to include a number of inequivalent atoms, thereby describing a larger *magnetic* and structural unit cell. In this sense, antiferromagnetism is a generalization of ferromagnetism and is a consequence of total-energy lowering due to more general magnetic sublattices. The resulting greater flexibility in spin arrangements can lead to nonmagnetic, ferromagnetic, antiferromagnetic, and ferrimagnetic solutions of the one-electron Kohn-Sham equations describing the system. Fixed-spin-moment calculations using two-atom magnetic unit cells have found[4,5] the volume range of existence of antiferromagnetic solutions for the 3*d* transition metals for bcc vanadium, chromium, and manganese, and fcc manganese and iron. In addition, ferrimagnetism is found for bcc manganese for a limited range of volumes. In the present work we extend the search for various forms of magnetic order in two-atom cells to the 4*d* transition metals and find antiferromagnetism for bcc niobium, molybdenum, and technetium, and for fcc technetium and ruthenium.

II. RESULTS

As in our work on the 3*d* transition metals, we use the fixed-spin-moment procedure[1] in combination with the nonrelativistic augmented-spherical-wave method of Williams, Kübler, and Gelatt,[6] which assumes a spherically ized potential within Wigner-Seitz spheres of radius r_{WS}. We use the local-spin-density approximation as formulated by von Barth and Hedin and modified by Janak[7] to account for exchange and correlation. Only collinear magnetism is considered.

Using the fixed-spin-moment procedure, we find the total energy E as a function of constrained magnetic moment M at a given volume V, or equivalently, at a given r_{WS}. The minima in the resulting function correspond to zero-field solutions of the Kohn-Sham equations at the given volume. The relative depth of multiple minima determines whether a zero-field solution is stable or metastable. Maxima in the $[E(M)]_V$ curve correspond to *unstable* zero-field solutions.

The results of a general survey of the equilibrium radii

TABLE I. Magnetovolume behavior of the 3d transition metals. Listed are equilibrium Wigner-Seitz radii, r_0, for critical radii for the onset of ferromagnetism, r_{FM}, order of nonmagnetic to ferromagnetic transitions (*C* refers to composite transitions), type (stable or unstable) of antiferromagnetic solutions, and critical radii for the onset of antiferromagnetism, r_{AF}, for 3d transition metals in the bcc and fcc structures.

System	r_0 (a.u.)	r_{FM} (a.u)	Order	Type	r_{AF} (a.u.)
bcc Sc	3.36	3.64	2		
fcc Sc	3.36	4.06	2		
bcc Ti	3.01	3.24	2		
fcc Ti	3.02	3.61	2		
bcc V	2.79	3.45	*C*	stable	3.15
fcc V	2.82	3.20	2		
bcc Cr	2.65	3.09	1	stable	2.72
fcc Cr	2.67	2.95	2		
bcc Mn	2.59	2.87	*C*	stable	2.70[a]
fcc Mn	2.58	2.83	1	stable	2.58
bcc Fe	2.62	2.27	2	unstable	
fcc Fe	2.54	2.66	*C*	stable[b]	2.54
bcc Co	2.60	2.25	2		
fcc Co	2.58	2.45	1		
bcc Ni	2.60	2.55	2		
fcc Ni	2.59	2.20	2		

[a]Ferrimagnetic.
[b]Up to 2.71 a.u.

and the onset of magnetic behavior for the 3d and 4d transition metals in both the bcc and fcc structures are summarized in Tables I and II. Here r_0, r_{FM}, and r_{AF} are Wigner-Seitz radii at equilibrium (zero pressure), at the onset of ferromagnetic behavior (ignoring low-spin solutions) as determined from one-atom-cell calculations, and at the onset of antiferromagnetic behavior as determined from two-atom-cell calculations, respectively. The transition from nonmagnetic to ferromagnetic behavior is classified as second order if the total energy and magnetic moment vary continuously with volume and show discontinuities only in the second derivative of the energy and the first derivative of the moment. A transition is first order if the total energy in the vicinity of the transition must be represented as two distinct curves and the magnetic moment shows a discontinuous jump in value.

TABLE II. Magnetovolume behavior of the 4d transition metals. Listed are equilibrium Wigner-Seitz radii, r_0, critical radii for the onset of ferromagnetism, r_{FM}, order of nonmagnetic to ferromagnetic transitions (*C* and *W* refer to composite and weak transitions, respectively), type (stable, metastable, or unstable) of antiferromagnetic solutions, and critical radii for the onset of antiferromagnetism, r_{AF}, for 4d transition metals in the bcc and fcc structures.

System	r_0 (a.u)	r_{FM} (a.u.)	Order	Type	r_{AF} (a.u.)
bcc Y	3.67	4.08	2		
fcc Y	3.66	4.70	2		
bcc Zr	3.27	3.90	2		
fcc Zr	3.31	4.27	2		
bcc Nb	3.07	4.28	*C*	stable	3.91
fcc Nb	3.11	3.90	2		
bcc Mo	2.95	3.86	1	stable	3.40
fcc Mo	2.96	3.76	2		
bcc Tc	2.88	3.64	*C*(*W*)	stable	3.50
fcc Tc	2.87	3.63	1(*W*)	stable	3.35
bcc Ru	2.86	2.99	2		
fcc Ru	2.83	3.46	1(*W*)	metastable	3.35
bcc Rh	2.86	3.23	1(*W*)		
fcc Rh	2.84[a]	3.24	1(*W*)	unstable	
bcc Pd	2.92	3.49	?(*W*)		
fcc Pd	2.91[a]	3.06	?(*W*)		

[a]The small differences between these values and those of Ref. 2 are due to details of the functional fit near the minimum.

Some systems undergo composite transitions (C) consisting of a second-order transition from nonmagnetic to low-spin behavior, followed by a first-order transition to high-spin ferromagnetic behavior. In addition, we classify a transition as weak (W) in cases where there is such a small range of coexistence of nonmagnetic and ferromagnetic behavior that we cannot resolve the energy curves, although the magnetic moment shows a discontinuous jump from zero to a finite value.

Our one-atom-cell fixed-spin-moment results are given by the tabulated r_{FM} values and the indicated order. In Table I we summarize previous[4,5] results and note that first-order or composite transitions from nonmagnetic to ferromagnetic behavior generally occur only in the middle of the transition series, and that two-atom-cell calculations usually yield antiferromagnetic solutions for these cases. Although cobalt in the fcc structure has a first-order transition, the differences between the nonmagnetic and ferromagnetic total energies and their volume derivatives are small; hence antiferromagnetic solutions may be difficult to locate. Note that we find *unstable* antiferromagnetic solutions for bcc iron although the nonmagnetic to ferromagnetic transition is second order.

As shown in Table II, yttrium and zirconium in both the bcc and fcc structure exhibit normal behavior. They are nonmagnetic at zero pressure and undergo second-order transitions to ferromagnetic behavior at the expanded volumes defined by the indicated r_{FM} values. Niobium and molybdenum in the fcc structure, and ruthenium in the bcc structure show similar behavior. The order of the transitions from nonmagnetic to ferromagnetic behavior for palladium in both the bcc and fcc structures is difficult to determine because the energy difference between nonmagnetic and magnetic behavior approaches the energy resolution in our calculations ($\simeq 0.02$ mRy/atom). These are weak transitions which appear[2] to be first order. The remaining systems, i.e., bcc niobium, molybdenum, technetium, and rhodium, and fcc technetium, ruthenium, and rhodium, all exhibit either first-order or composite transitions, and are candidates for antiferromagnetic behavior.

A. Niobium

As listed in Table II, bcc niobium in a one-atom-cell description exhibits a composite transition from nonmagnetic to ferromagnetic behavior. The composite nature of this transition is a consequence of the existence of low-spin (LS) ferromagnetic solutions at volumes just below the onset of high-spin ferromagnetic behavior. The details of this transition are seen in Fig. 1, where we show zero-field total energy and magnetic moment results for this system. The one-atom-cell (bcc) results are labeled NM (nonmagnetic), LS (low-spin), and FM (ferromagnetic). Our two-atom-cell (CsCl) results are labeled AF (antiferromagnetic). The one-atom-cell calculations show that bcc niobium is nonmagnetic in the ground state (at the energy minimum) and undergoes a composite transition (with a range of low-spin behavior) to ferromagnetic behavior at $r_{FM} \simeq 4.28$ a.u. However, for $r_{WS} > 3.91$ a.u., the two-atom-cell calculations yield antiferromagnetic order with lower total energies than either low-spin or high-spin ferromagnetic order. Note that the transition to antiferromagnetism is second order, and the total energy curve for antiferromagnetism blends smoothly with the nonmagnetic (or low-spin) curve at lower volumes, and also tends towards the high-spin ferromagnetic curve at higher volumes. Antiferromagnetism is energetically more favorable and apparently offers a more gradual way for the system to undergo a transition from nonmagnetic to magnetic behavior. This general behavior is found for almost all transition metals which exhibit first-order transitions when constrained to a one-atom-cell description.

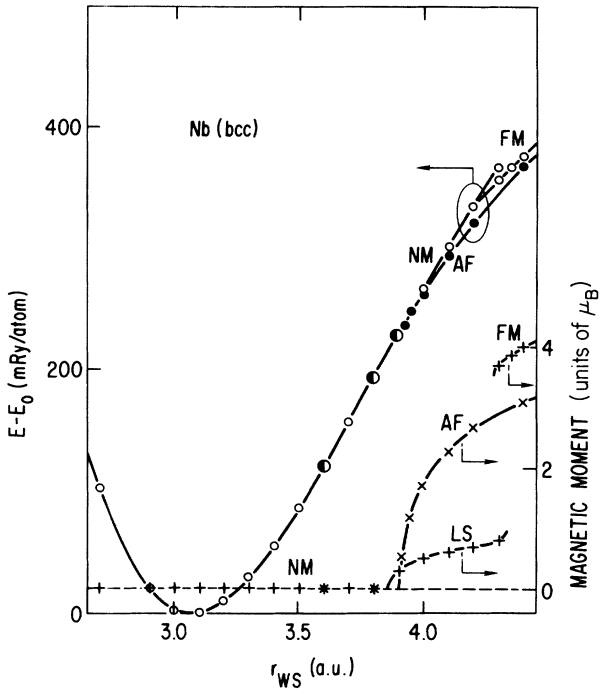

FIG. 1. Zero-field total energy and magnetic moment vs r_{WS} for bcc niobium showing one-atom-cell nonmagnetic (NM), low-spin (LS), and ferromagnetic (FM) solutions, and two-atom-cell antiferromagnetic (AF) solutions. One-atom-cell (bcc) total energies are shown as open circles and magnetic moments as + symbols. Two-atom-cell (CsCl) total energies are shown as solid circles and local moments as × symbols. The larger half-solid circles and the combination + and × symbols represent identical one-atom- and two-atom-cell results. The reference energy E_0 is the energy minimum for the nonmagnetic state.

B. Molybdenum

In Fig. 2 we show the zero-field total energy and magnetic moment results for one-atom and two-atom-cell solutions for molybdenum constrained to bcc and CsCl lattices. The one-atom-cell (bcc) results show an onset of ferromagnetic behavior via a first-order magnetovolume transition at $r_{WS} \simeq 3.86$ a.u., with a range of coexistence for both nonmagnetic and ferromagnetic behavior extending to $r_{WS} \simeq 4.00$ a.u. Two-atom-cell (CsCl) calculations, however, show that antiferromagnetic solutions are energetically more favored for $r_{WS} > 3.40$ a.u., and that

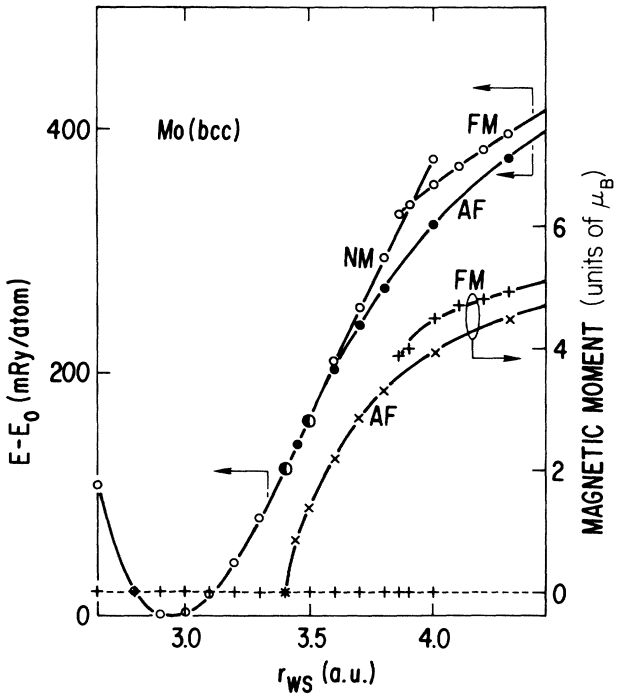

FIG. 2. Zero-field total energy and magnetic moment vs r_{WS} for bcc molybdenum showing one-atom-cell nonmagnetic (NM) and ferromagnetic (FM) solutions, and two-atom-cell antiferromagnetic (AF) solutions. The reference energy E_0 is the energy minimum for the nonmagnetic state. See Fig. 1 for explanation of symbols.

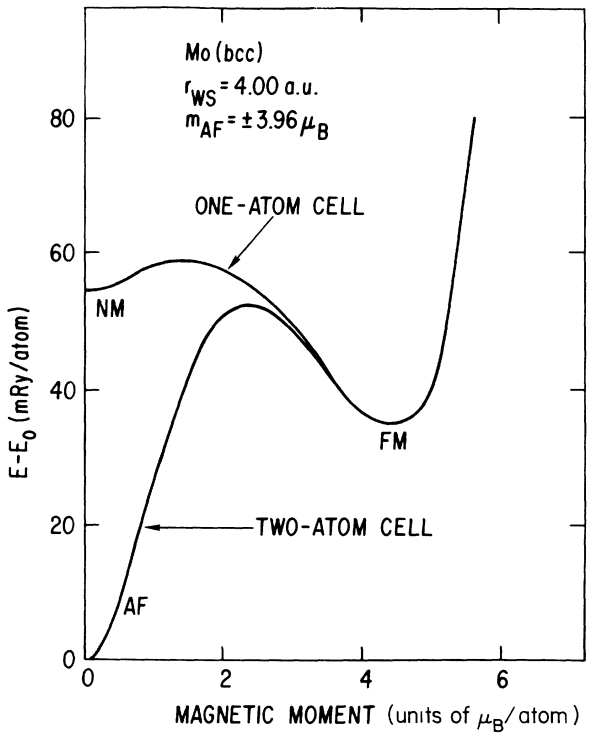

FIG. 3. One-atom-cell and two-atom-cell energy vs average moment per atom for bcc molybdenum at $r_{WS}=4.00$ a.u. The minima locate zero-field solutions which are either stable or metastable. The nonmagnetic (NM) one-atom-cell solution is metastable relative to the other zero-field solutions shown. The ferromagnetic (FM) solution at $M\simeq 4.5\mu_B$/atom is observed for both the one-atom-cell and two-atom-cell calculations. Note that the "stable" FM one-atom-cell solution is metastable relative to the AF two-atom-cell solution. The local antiferromagnetic moments, m_{AF}, at $M=0$ for the two-atom-cell calculation are $\pm 3.96\mu_B$.

the transition from nonmagnetic to antiferromagnetic behavior is second order; the antiferromagnetic total energy merges smoothly with the nonmagnetic total energy at low volumes and tends towards the ferromagnetic total energy at large volumes, similar to the bcc niobium case. This general behavior is also consistent with our 3d results and our observation[4] that first-order magnetovolume transitions tend to be suppressed by increasing the size of the magnetic cell.

A typical energy versus moment curve for this system is displayed in Fig. 3, where we show the calculated total energy versus magnetic moment for a volume corresponding to $r_{WS}=4.00$ a.u. One-atom-cell calculations yield the metastable nonmagnetic solution labeled NM and the stable ferromagnetic solution labeled FM. However, two-atom-cell calculations show that the ferromagnetic solution is actually metastable relative to the antiferromagnetic solution labeled AF. Since the two curves are calculated with different sets of points in k space, the merging of the two curves at large moments implies k-space convergence. Note that the zero *total* moment for this antiferromagnetic solution is a consequence of the cancellation of *local* moments of $\pm 3.96\mu_B$. Thus the zero-field local antiferromagnetic moments, m_{AF}, equal $\pm 3.96\mu_B$.

C. Technetium

Although technetium is radioactive and does not occur naturally, it can be treated theoretically as readily as the other transition metals. Since it is isoelectronic to manganese, it can be expected to show similar behavior. In Fig. 4 we show our one-atom- and two-atom-cell zero-field total-energy and magnetic-moment results for this element constrained to the bcc and CsCl lattices. This system resembles bcc niobium; it exhibits nonmagnetic, low-spin, and ferromagnetic one-atom-cell solutions, and antiferromagnetic two-atom-cell solutions. We describe the transition from nonmagnetic to ferromagnetic behavior as weak because of the negligible coexistence region. In the energy curves, this transition is barely detectable as a discontinuity in derivative at $r_{WS}\simeq 3.64$ a.u. The most striking difference from niobium is that the transition from nonmagnetic to antiferromagnetic behavior is first order. This system is therefore similar to bcc chromium,[5] and may be expected to have a complicated many-atom antiferromagnetic cell at expanded volumes. Note that the antiferromagnetic total energy merges smoothly with the ferromagnetic total energy at large volume, although the antiferromagnetic and ferromagnetic local moments are unequal.

Zero-field results for technetium constrained to fcc and CuAu lattices are shown in Fig. 5. One-atom-cell calcu-

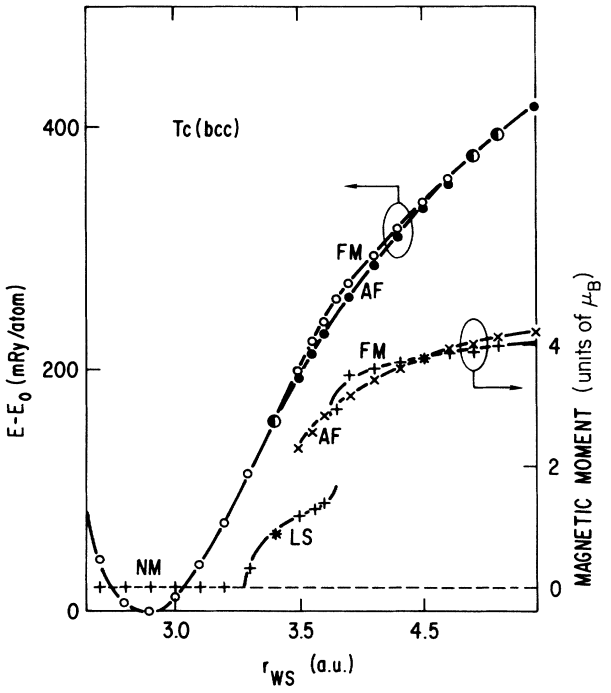

FIG. 4. Zero-field total energy and magnetic moment vs r_{WS} for bcc technetium showing one-atom-cell nonmagnetic (NM), low-spin (LS), and ferromagnetic (FM) solutions, and two-atom-cell antiferromagnetic (AF) solutions. The reference energy E_0 is the energy minimum for the nonmagnetic state. See Fig. 1 for explanation of symbols.

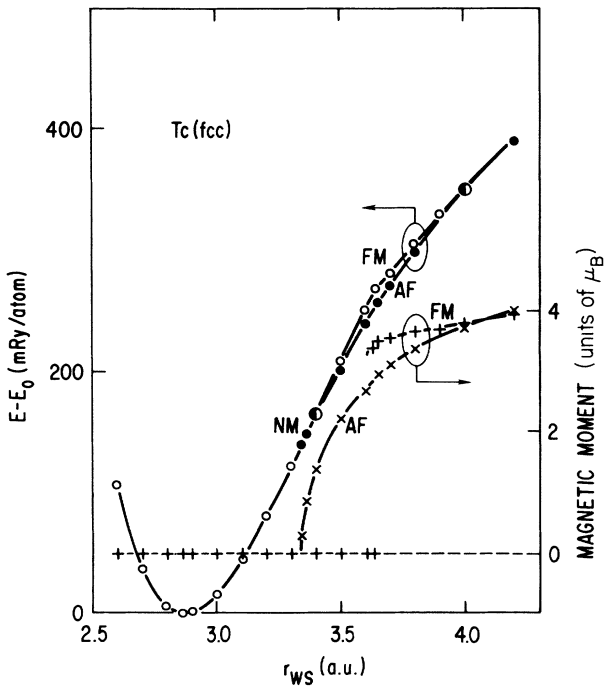

FIG. 5. Zero-field total energy and magnetic moment vs r_{WS} for fcc technetium showing one-atom-cell nonmagnetic (NM) and ferromagnetic (FM) solutions, and two-atom-cell antiferromagnetic (AF) solutions. The reference energy E_0 is the energy minimum for the nonmagnetic state. See Fig. 1 for explanation of symbols.

lations show a first-order magnetovolume transition from nonmagnetic to ferromagnetic behavior at $r_{WS} \simeq 3.63$ a.u. with a very small coexistence range. The two-atom-cell CuAu calculations, however, show energetically favored antiferromagnetic solutions extending down to $r_{WS} \simeq 3.35$ a.u. Note that the first-order magnetovolume transition found in the one-atom-cell calculation is replaced by a second-order transition in the two-atom-cell calculation and that the energies involved in the latter are lower. In addition, the onset of magnetic behavior occurs at lower volumes. Again, the antiferromagnetic total energies merge smoothly with the nonmagnetic total energies at low volumes and tend towards the ferromagnetic total energies at large volumes.

Typical energy versus magnetic-moment curves for one-atom- and two-atom-cell calculations for this system for $r_{WS} = 2.70$ a.u. are shown in Fig. 6. The most stable zero-field solution is seen to be the two-atom-cell antiferromagnetic solution with $m_{AF} = \pm 3.11 \mu_B$. The ferromagnetic solution at $r_{WS} \simeq 3.5 \mu_B$/atom, found in both calculations, is now metastable.

D. Ruthenium

Although ruthenium might be expected to be similar to iron, it does not form in the bcc structure, and is not magnetic in the ground state. As shown in Fig. 7, fcc ruthenium constrained to a one-atom-cell description be-

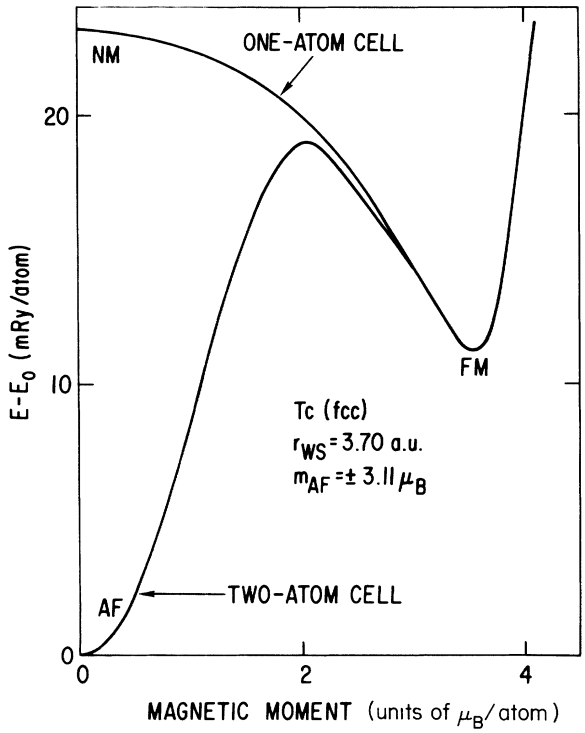

FIG. 6. One-atom-cell and two-atom-cell energy vs average moment per atom for fcc technetium at $r_{WS} = 3.70$ a.u. The "stable" ferromagnetic (FM) one-atom-cell solution becomes metastable when a two-atom-cell is considered. The local antiferromagnetic moments at $M = 0$ for the two-atom cell, m_{AF}, are $\pm 3.11 \mu_B$.

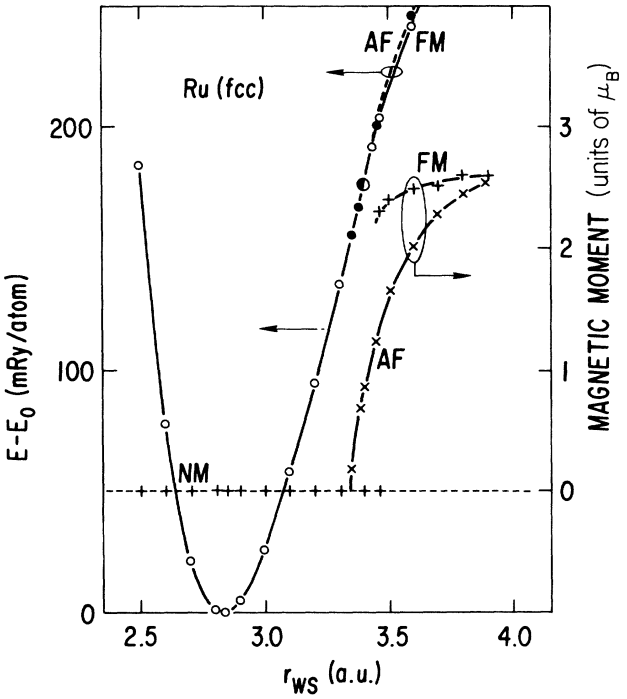

FIG. 7. Zero-field total energy and magnetic moment vs r_{WS} for fcc ruthenium showing one-atom-cell nonmagnetic (NM) and ferromagnetic (FM) solutions, and two-atom-cell antiferromagnetic (AF) solutions. The antiferromagnetic total energy branch is shown dashed to distinguish it from the ferromagnetic branch. The reference energy E_0 is the energy minimum for the nonmagnetic state. See Fig. 1 for explanation of symbols.

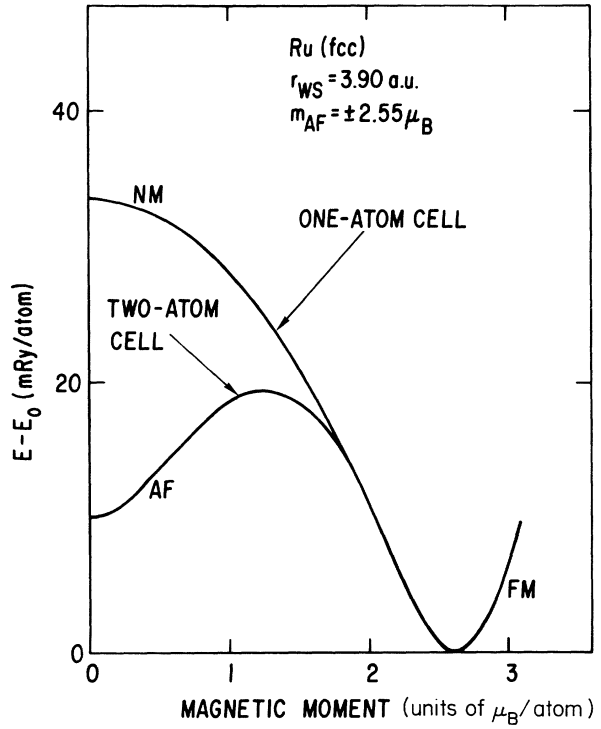

FIG. 8. One-atom-cell and two-atom-cell energy vs average moment per atom for fcc ruthenium at $r_{WS}=3.90$ a.u. The antiferromagnetic (AM) two-atom-cell solution with local moments at $M=0$ of $m_{AF}=\pm 2.55\mu_B$ remains metastable relative to the ferromagnetic (FM) solution displayed by both the one-atom- and two-atom-cell calculations.

comes ferromagnetic at $r_{WS}\simeq 3.46$ a.u. via a "weak" first-order transition. In a two-atom-cell description, we find a range of antiferromagnetic solutions beginning at $r_{WS}\simeq 3.35$ a.u. These solutions, however, are energetically less favorable than the ferromagnetic solutions, and are classified as metastable. Again, the first-order transition from nonmagnetic to ferromagnetic behavior obtained in the one-atom-cell calculation is replaced by a second-order transition from nonmagnetic to antiferromagnetic behavior in the two-atom-cell calculation.

The relative stability of the zero-field ferromagnetic and antiferromagnetic solutions can be inferred from $[E(M)]_V$ curves like Fig. 8, which shows energy versus magnetic moment derived from one-atom- and two-atom-cell calculations for $r_{WS}=3.90$ a.u. As shown, the zero-field antiferromagnetic solution with $m_{AF}=\pm 2.55\mu_B$ is metastable relative to the ferromagnetic solution at $M\simeq 2.6\mu_B$. This relative metastability persists throughout the range corresponding to $r_{WS}>3.46$ a.u., demonstrating that although two-atom-cell calculations generally allow for more flexible spin arrangements and lower energies, the energy lowering may be limited to certain moment ranges.

III. DISCUSSION

We have shown that bcc niobium, molybdenum, and technetium, and fcc technetium and ruthenium, all show first-order transitions from nonmagnetic to ferromagnetic behavior in a one-atom-cell description, and that these same systems show transitions to antiferromagnetism at appreciably lower volumes in a two-atom-cell description. Whenever a first-order magnetovolume transition to ferromagnetism is found, the system will usually undergo a more gradual second-order transition to antiferromagnetic behavior at lower volumes. Chromiun, manganese, and technetium in the bcc structure offer the possibility of additional complications; i.e., in two-atom-cell descriptions they still exhibit first-order transitions to antiferromagnetism. Hence it is plausible that in appropriate many-atom-cell descriptions, i.e., more than two-atom cells, these elements will follow the same rule and undercut the first-order transitions by more suitable second-order transitions.

This replacement of first-order transitions by second-order transitions occurs in both the 3d and 4d transition metals. The antiferromagnetic total energies generally merge smoothly[8] with nonmagnetic or low-spin total energies at low volumes, and tend towards the ferromagnetic total energies at large volumes. Thus, as the volume or the atomic separation increases, the energy difference between parallel and antiparallel spin arrangements decreases. We note that (type I) antiferromagnetic fcc systems are expected[9] to undergo tetragonal distortions, which lower the total energy.

Rhodium and palladium in the fcc structure undergo

"weak" first-order transitions from nonmagnetic to ferromagnetic behavior in the sense noted above, i.e., exhibiting small coexistence ranges of nonmagnetic and ferromagnetic solutions. Attempts to find stable antiferromagnetic solutions for these systems have thus far been unsuccessful. We find that rhodium in the fcc structure at $r_{WS}=3.60$ a.u. does have an antiferromagnetic solution with local moments of $\pm 0.7\mu_B$, but that this solution is unstable with respect to the ferromagnetic solution, similar to the unstable antiferromagnetic solution seen for bcc iron. One-atom-cell calculations for rhodium and palladium yield transitions from nonmagnetic to ferromagnetic behavior that appear to be first order. However, the energy changes are so small that we do not resolve the break in the slopes of the energy curves at the transition volumes. Hence we do not find the usual accompanying concavity of the composite energy curve, which is then bridged by the more gradual antiferromagnetic transitions. If stable antiferromagnetic solutions exist, they lie very close to the ferromagnetic solutions and are difficult to resolve. We note, however, that rhodium and palladium[2] have magnetic moments that *exceed* the free-atom Hund's-rule limit even at the onset of ferromagnetism, and therefore may be different from other transition metals.

In summary, our survey of the occurrence of antiferromagnetism in the 4*d* transition metals in two-atom cells reveals four cases with stable antiferromagnetic solutions—bcc niobium, molybdenum, and technetium and fcc technetium; one case with metastable antiferromagnetic solutions—fcc ruthenium; and one case with unstable antiferromagnetic solutions—fcc rhodium. As summarized in Table II, we note that all of the stable solutions occur near the center of the series, and that they favor bcc structures at the lower end and fcc structures at the upper end. In addition, antiferromagnetism in the 4*d* series tends to occur at volumes further removed from equilibrium than in the 3*d* series.

Finally, we conclude from our survey of the magnetic properties of the 3*d* and 4*d* transition metals over extended volumes that the tendency for antiferromagnetism is weaker in the 4*d* than in the 3*d* series. Although we find five cases of stable or metastable antiferromagnetic solutions in each series (out of the 16 possible cubic structures in each series), the antiferromagnetic transition occurs within 5% of the equilibrium volume in four of the five cases in the 3*d* series, but requires a lattice expansion of at least 15% in all of the cases in the 4*d* series. Moreover, for chromium and manganese, the experimental ground state actually has local magnetic moments that vary from atom to atom within magnetic cells that contain more than two atoms.

[1]A. R. Williams, V. L. Moruzzi, J. Kübler, and K. Schwarz, Bull. Am. Phys. Soc. **29**, 278 (1984).

[2]V. L. Moruzzi and P. M. Marcus, Phys. Rev. B **39**, 471 (1989).

[3]For a general survey of magnetovolume transitions in the 3*d* transition metals, see V. L. Moruzzi and P. M. Marcus, Phys. Rev. B **38**, 1613 (1988), and references therein.

[4]V. L. Moruzzi, P. M. Marcus, and J. Kübler, Phys. Rev. B **39**, 6957 (1989); V. L. Moruzzi and P. M. Marcus, Solid State Commun. **71**, 203 (1989).

[5]V. L. Moruzzi and P. M. Marcus, Phys. Rev. B **42**, 8361 (1990).

[6]A. R. Williams, J. Kübler, and C. D. Gelatt, Jr., Phys. Rev. B **19**, 6094 (1979).

[7]U. von Barth and L. Hedin, J. Phys. C **5**, 1692 (1972); J. F. Janak, Solid State Commun. **25**, 53 (1978).

[8]A discontinuous derivative in $E(r_{WS})$ at the antiferromagnetic transition is observed for bcc Cr, Mn, and Tc.

[9]T. Oguchi and A. J. Freeman, J. Magn. Magn. Mater. **46**, L1 (1984).